ARCHIVES
of
FOUNDRY ENGINEERING

ISSN (2299-2944)

10.24425/afe.2025.155375

Published quarterly as the organ of the Foundry Commission of the Polish Academy of Sciences

Cavitation erosion resistance tests of WCCoCr and CrCNi coatings sprayed using the APS method

M. Radoń *, B. Kupiec
Rzeszow University of Technology, Poland
* Corresponding author: E-mail address: m.radon@prz.edu.pl

Received 03.03.25; accepted in revised form 14.07.25; available online 27.10.2025

Abstract

This article presents structural analysis and mechanical property evaluation of two coatings applied using the APS (Air Plasma Spraying) method on a P250GH boiler steel substrate. Two different powders were used for coating deposition: WCCoCr, based on tungsten carbide, and CrCNi, based on chromium carbide.
To assess the coating-substrate bond quality, a scratch test was conducted using a Rockwell diamond indenter under a constant load of 10 N, moving from the substrate toward the coating. No delamination at the coating-substrate interface was observed, indicating a high-quality bond.
Microhardness measurements were performed using a 200 g load. The average microhardness values were 886 HV0.2 for the WCCoCr coating and 904 HV0.2 for the CrCNi coating.
The coatings were also tested for cavitation resistance according to the ASTM G32-16 standard. Surface roughness profiles were measured before and after 120 minutes of cavitation exposure.
Cavitation wear was evaluated based on the difference in roughness values, determined by the S_z parameter, which, according to ISO 25178, is defined as the difference between the highest peak and the lowest valley on the surface.
The obtained results indicate that APS thermal spray coatings based on tungsten carbide powders can be used for machine components to enhance cavitation erosion resistance.

Keywords: Air plasma spraying coating, Scratch test, Cavitation erosion

1. Introduction

Modifying the surface layer of machine components. It is applied to enhance wear resistance, improve corrosion resistance, and extend the service life of components operating at high temperatures. Coatings are also used for component regeneration and restoring desired dimensions [1].

The selection of the most suitable coating is primarily achieved by altering the base material (powders) and choosing the appropriate thermal spraying process. To obtain hard coatings resistant to abrasive, cavitation, or erosive wear, powder manufacturers offer innovative combinations of hard particles within a softer matrix. Cavitation erosion is a common phenomenon in hydraulic components such as hydraulic pumps, diesel engines, valves, and propellers, which are often made of metallic or alloy materials [2]. During operation, these components frequently come into contact with vibrating or fast flowing liquids under variable pressure conditions. The pressure fluctuations cause

the formation and collapse of vapor bubbles, generating stress impulses on nearby solid surfaces, leading to erosion [3].

Applying suitable coatings to working components is often necessary to extend their service life. For example, WC-based coatings can be used to enhance resistance to wear, oxidation, and erosion-corrosion [4,5].

Hard coatings made of cemented carbides are commonly applied using HVOF (High-Velocity Oxygen Fuel), HVAF (High-Velocity Air Fuel), APS (Air Plasma Spraying), and CDS (Detonation Spray) methods [6,7].

According to [8],coatings produced by the HVAF process demonstrated lower porosity and oxide content, as well as higher hardness values compared to those sprayed by HVOF. HVAF-sprayed coatings exhibited improved cavitation and corrosion resistance. In contrast, for HVOF coatings, the presence of oxides and porosity played a critical role in their corrosion performance, as they facilitated the penetration of chloride ions through pores, leading to accelerated corrosion and pit formation.

In the study [9], Al_2O_3–TiO_2 coatings produced by APS and S-HVOF (Suspension High Velocity Oxy-Fuel) processes were investigated to assess the influence of spraying technology and feedstock characteristics.

The coatings were characterized in terms of selected mechanical properties and wear resistance, including fracture toughness, Vickers hardness, and nanoindentation-derived parameters such as instrumental hardness and Young's modulus, as well as sliding and cavitation erosion resistance. The authors found that homogeneous S-HVOF coatings demonstrated superior mechanical properties compared to those sprayed by APS.

Coating porosity depends on the spraying method, process parameters, and the nature of the feedstock (powder or wire), as also confirmed by [10], who reported that porosity levels in APS-sprayed coatings may range from below 2 vol.% to over 20 vol.%.

Feedstock materials vary in chemical composition and particle morphology. The most common powder manufacturing technique is atomization, where a stream of molten metal is broken into fine droplets using a high-pressure atomizing medium such as water, steam, air, or inert gas [11].

The final coating quality is also influenced by the selected process parameters and substrate preparation before spraying [12,13]. According to some authors [14], more than 50 macroscopic parameters can affect coating quality.

Authors in studies [15,16] have demonstrated that the use of chromium carbide-based coatings (e.g., Cr_3C_2–50NiCrMoNb) can significantly improve corrosion resistance due to the higher content of Ni625-based metallic matrix.

The aim of this study was to evaluate the applicability of APS-sprayed coatings produced from tungsten carbide-based (WCCoCr) and chromium carbide-based (CrCNi) powders in enhancing the cavitation erosion resistance of components. The analysis included microstructural examination, microhardness measurements, and degradation resistance under severe cavitation loading, in order to assess the potential of these coatings for extending the service life of components operating in demanding environments.

2. Material and Research Methodology

The substrate material consisted of P250GH steel plates (Table 1) with dimensions of 50 × 25 × 4 mm.

Table 1.
Results of the chemical composition analysis of the P250GH steel, weight %

C	Si	Mn	Cr	Mo	Cu	Al	Fe
0.17	0.012	0.9	0.02	0.015	0.019	0.05	rest

Before the spraying process, the surface of the plates was degreased with acetone and then subjected to sandblasting with electrocorundum in an air stream under a pressure of 6 bar. The nozzle was held at a distance of approximately 1000 mm from the surface of the plates. The average value of the height parameter S_z (the difference in height between the peak line and the valley line) for the prepared surface of the plates was 28 µm.

Two powders were used to create the coatings: WCCoCr based on tungsten carbide and CrCNi based on chromium carbide. According to the manufacturer's data, the chemical composition of the WCCoCr powder contained 42% W, 34% Cr, 20% Co, and 4% C, with particle sizes of - 45µm/+16µm. The CrCNi powder contained 88% Cr, 8% Ni, and 4% C, with particle sizes of -53µm/+16µm. Both powder variants were produced by atomization.

For microanalysis of the powder particles chemical composition, a Tescan VEGA scanning electron microscope equipped with an INCA x-act chemical composition analysis attachment from Oxford Instruments was used. The images of the powder particles used in the APS thermal spraying process along with the microanalysis of their chemical composition are shown on Figures 1 and 2.

The plasma spraying process was carried out on a robotic station SULZER METCO, equipped with an ABB robot, F4-MB-HBS burner, and an integrated powder feeder. Table 2 summarizes the developed technological parameters for the APS spraying process of powders onto a P250GH steel substrate.

The microstructure studies were conducted on metallographic sections obtained by polishing cut and embedded plates with coatings, each 4 mm in width. The coating thickness was assessed using a TESCAN Vega 3 scanning electron microscope.

Microhardness evaluation (HV0.2) of the coatings was carried out using a ZHVm Indentec microhardness tester from Zwick/Roell. The results represent the average of ten measurements, taken at the midpoint of the coating thickness. The load for the hardness measurements was selected to ensure that all microstructural components present in the coating were included within the indentation area.

The quality of the coating-substrate bond was evaluated using the REVETEST RST device. The Rockwell diamond indenter moved from the P250GH steel substrate toward the coating, under a constant load of 10 N. The indenter's movement speed was 0.5 mm/min.

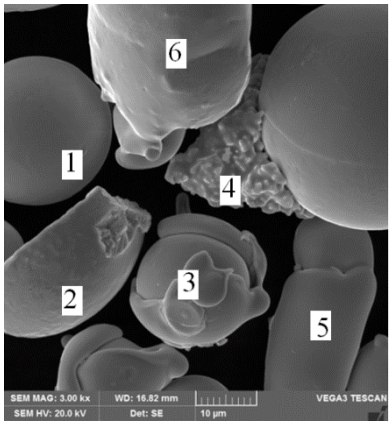

Point	C	Cr	Co	W
1	4.36	33.96	19.82	41.86
2	2.27	42.14	27.37	28.22
3	4.67	34.05	19.93	41.35
4	3.52	37.94	24.95	33.59
5	4.31	39.38	22.88	33.42
6	2.56	44.08	27.00	26.36

Fig. 1. Example view of WCCoCr powder particles with chemical composition microanalysis

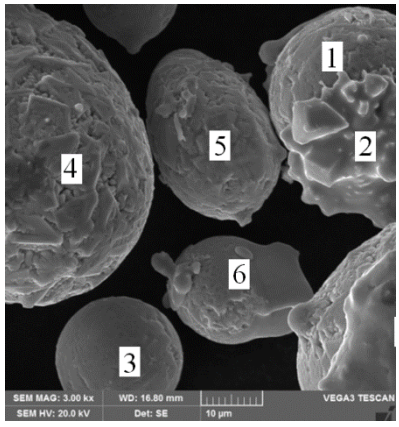

Point	C	Cr	Ni
1	7.15	83.21	9.64
2	5.37	85.37	9.26
3	2.67	94.74	2.59
4	7.19	84.95	7.87
5	5.33	85.55	9.11
6	6.53	85.67	7.79

Fig. 2. Example view of CrCNi powder particles with chemical composition microanalysis

Cavitation wear tests were conducted on a VCX 130 Sonicator. The coated samples were polished using sandpapers with grit sizes of 600 and 1000. The average value of the S_z parameter (the difference between the highest peak and the lowest valley on the surface) for the WCCoCr coating in the initial state was 15.2 µm, while for the CrCNi coating, it was 23.4 µm.

Table 2.
Technological parameters of plasma spraying coatings on P250GH plates

Parameter	WCCoCr	CrCNi
Carrier gas, l/min:	4	4
Powder feeder disk speed, rpm:	0.9	0.9
Current intensity, A:	650	650
Argon flow rate, l/min:	55	60
Hydrogen flow rate, l/min:	7	7
Air jet pressure, bar:	3	3
Spraying distance, mm:	115	115
Linear velocity of the torch, mm/min:	175	175
Number of torch passes:	23	19

An example of a 3D surface view and a 2D roughness profile passing through the center of the surface are presented in Figures 3 and 4.

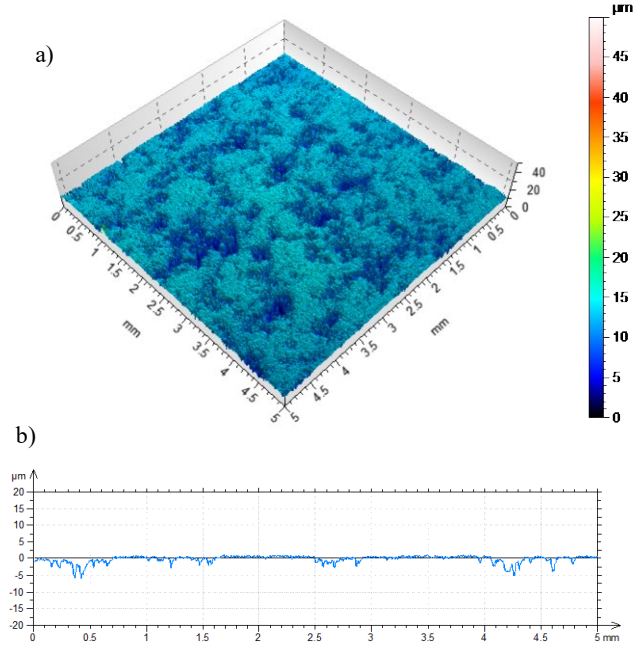

Fig. 3. Example view of a 3D surface and a 2D roughness profile of the WCCoCr coating before cavitation resistance testing

Cavitation erosion resistance tests were carried out in accordance with ASTM G32-16 (Standard Test Method for Cavitation Erosion Using Vibratory Apparatus), using the indirect method (Method B), in which the specimen does not come into direct contact with the sonotrode. Cavitation is generated within the liquid gap between the tip of the sonotrode and the surface of the specimen.

The tests were conducted using an ultrasonic generator operating at a frequency of 20 ± 1 kHz. The vibration amplitude of the sonotrode tip was maintained at a level compliant with the standard requirements and verified by means of a stroboscopic method.

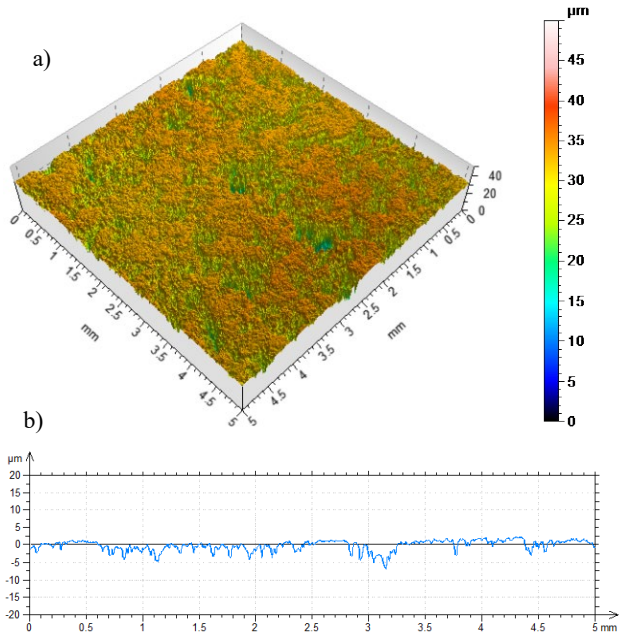

Fig. 4. Example view of a 3D surface and a 2D roughness profile of the CrCNi coating before cavitation resistance testing

The distance between the sonotrode tip and the specimen surface was set to 0.5 ± 0.05 mm. The specimens were placed in a vessel filled with distilled water as the working fluid. The temperature of the fluid was maintained at 25 ± 2°C throughout the entire test duration. The measure of cavitation wear was the difference in surface roughness values of the samples in the initial state and after 120 minutes of cavitation.

3. Results

Example microstructures of the WCCoCr and CrCNi thermally sprayed coatings are presented in Figures 5-6.

The selection of technological parameters for the APS spraying process enabled the production of coatings with appropriate thicknesses within the specified range. The thickness of the tungsten carbide-based coating was 348 µm, while the chromium carbide-based coating measured 403 µm. In both coatings, the presence of oxides and microcracks was observed, with a higher number of microcracks detected in the CrCNi coating.

The APS-sprayed powders on the P250GH steel substrate formed coatings with a characteristic lamellar structure, typical for such materials.

The coatings produced exhibited low porosity, with 3% for the WCCo coating and 6.3% for the CrCNi coating.

Porosity assessment was performed on metallographic sections using a scanning electron microscope (SEM) at a 2000x magnification. For each coating, three randomly selected areas, each with a surface area of 8262 µm², were analyzed.

Microhardness testing results revealed that the average microhardness value of the WCCoCr coating was 886 HV0.2, while the CrCNi coating had an average of 904 HV0.2.

Figure 7 shows an example of a scratch test in the coating-substrate transition area for the WCCoCr coating, while the scratch test in the coating-substrate transition area for the CrCNi coating is shown in Figure 8.

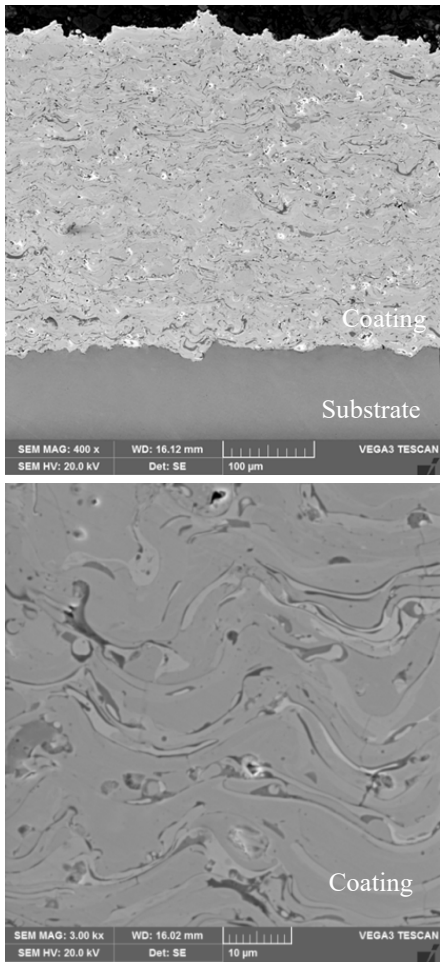

Fig. 5. Example view of the WCCoCr coating thermally sprayed using the APS method on a P250GH steel substrate, with an average thickness of 348 µm

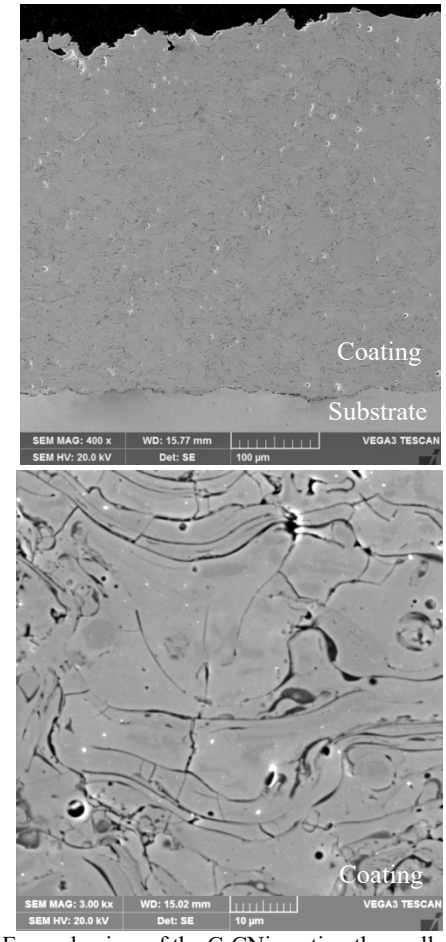

Fig. 6. Example view of the CrCNi coating thermally sprayed using the APS method on a P250GH steel substrate, with an average thickness of 403 µm

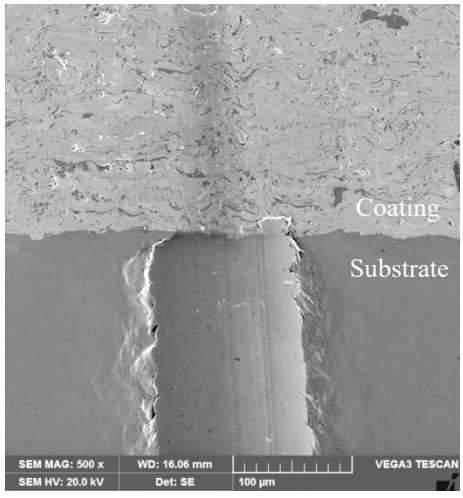

Fig.7. View of the scratch test in the coating-substrate transition area of the WCCoCr coating

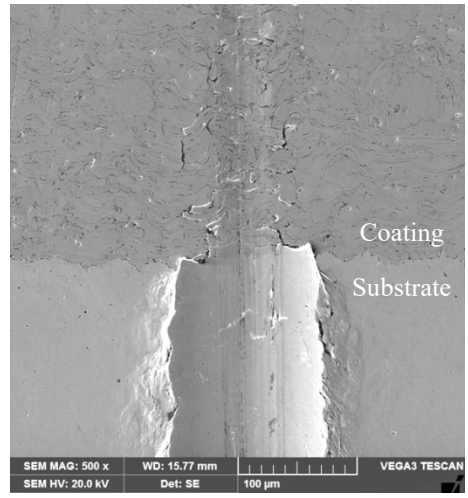

Fig.8. View of the scratch test in the coating-substrate transition area of the CrCNi coating

The obtained results indicate good bonding quality between the coatings and the substrate material. No delamination was observed in the indenter transition area at this boundary. Surface analysis of the scratch in the coating revealed only microcracks between/within the splats. According to [17], each layer of the coating forms as a result of high-speed particle impacts undergoing a rapid solidification process. Therefore, the coatings exhibit an elongated splat morphology with varying curvature and porosity.

As a result, a network of microcracks forms between/within the splats, leading to a variable microstructure of the coating and slightly differing mechanical properties [18-19]. The resulting differences mainly depend on the characteristics of the plasma stream, the condition of the substrate, and the positioning of the powder feed nozzle during the spraying process. The quality of substrate preparation (roughness) is one of several variables during thermal spraying that affects splat formation [20-21].

Example surfaces of the WCCoCr and CrCNi coatings, along with roughness profiles passing through the centers of the formed craters, are shown in Figures 9 and 10.

3D maps and 2D roughness profiles were complemented with macro- and microscopic views of these surfaces using a scanning electron microscope (Figures 11, 12). To reveal the entire circumference of the cavitation interaction surface, a magnification of 30x was used. Views of representative micro-areas were taken with a thousandfold magnification. Table 3 presents the values of the S_z parameter for the surface's geometric structure in the cavitation interaction area of the tested surfaces, along with the diameter of the cavitation erosion area.

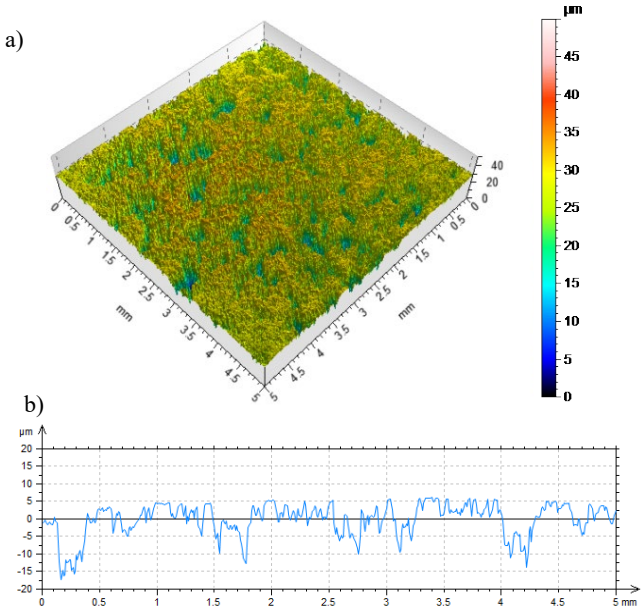

Fig. 9. Example view of the 3D surface and 2D roughness profile of the WCCoCr coating after cavitation resistance testing

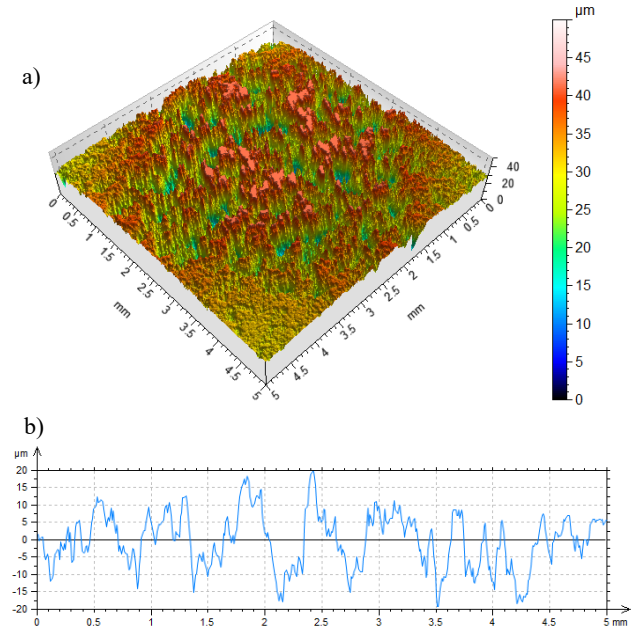

Fig. 10. Example view of the 3D surface and 2D roughness profile of the CrCNi coating after cavitation resistance testing

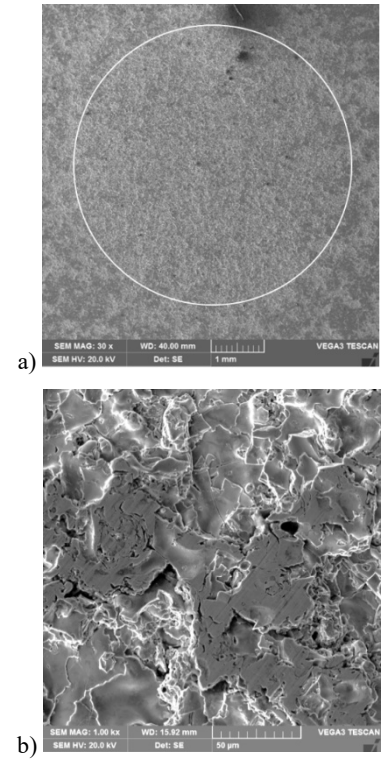

Fig. 11. The cavitation interaction area on the WCCoCr coating (a), and an exemplary view of the surface (b)

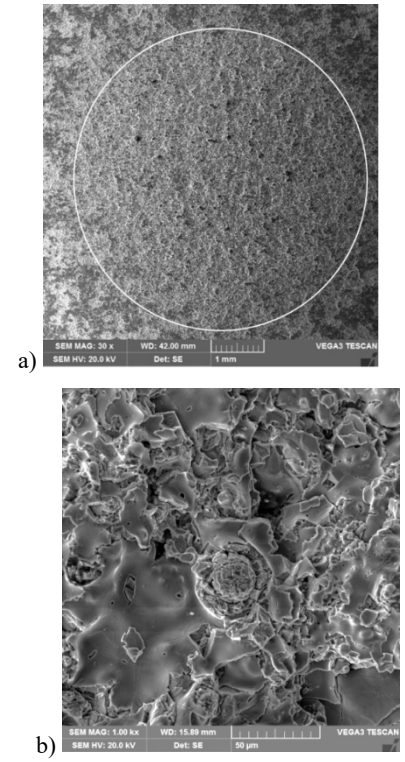

Fig. 12. The cavitation interaction area on the CrCNi coating (a) and an exemplary view of the surface (b)

Table 3.
Values of the S_z parameter of the surface geometry in the cavitation interaction area of the tested surfaces and the diameter of the cavitation erosion area

Material	The value of the parameter S_z, µm		The value of the difference in the S_z parameter before and after testing, µm
	before cavitation	after cavitation	
WCCoCr coating	15,2	26,5	11,3
CrCNi coating	23,4	39,6	16,2

The analysis of the surface geometry of the tested materials indicates that the coating produced from tungsten carbide exhibits lower cavitation wear compared to the chromium carbide-based coating.

This enhanced performance can be attributed to the superior cohesive properties of the characteristic lamellar structure observed in the WC-based coating. These properties are likely associated with a lower oxide content and a reduced number of microcracks between splats, resulting in a more compact and mechanically stable microstructure.

Furthermore, the reduced presence of oxides at splat boundaries in the WCCoCr coating likely minimizes weak interfaces that are susceptible to cavitation-induced stress concentration and crack initiation. In contrast, the CrCNi coating may have a higher degree of interlamellar oxidation and microcrack formation, which compromises structural integrity under dynamic fluid loading.

Additionally, the denser and more homogeneous microstructure of the WC-based coating could enhance load distribution during cavitation bubble collapse events, thereby delaying surface fatigue and material removal. These findings suggest that the WCCoCr coating may be more suitable for applications involving intensive cavitation conditions, especially where long-term resistance and structural durability are critical.

4. Conclusions

Cavitation occurs in various components of machines and hydraulic equipment, where the working fluid moves at high velocities and under fluctuating pressure conditions. The components most exposed to cavitation include pump and turbine blades, impellers, valves, flow sleeves, fluid inlets/outlets, baffles, and other flow-exposed surfaces.

Based on the presented research, the following conclusions can be drawn:

The WCCoCr coating demonstrates significantly higher resistance to cavitation wear compared to the CrCNi coating. This is confirmed by surface roughness changes observed after the cavitation erosion test. The difference in the Sz parameter within the cavitation-affected area was 11.3 µm for the WCCoCr coating and 16.2 µm for the CrCNi coating.

The superior resistance of the WCCoCr coating may result from its characteristic lamellar structure, which exhibits higher cohesion, fewer microcracks between splats, lower oxide content, and reduced porosity compared to the CrCNi coating. These features may help limit and delay the initiation of cracks caused by the implosion of cavitation bubbles.

The denser and more compact microstructure of the WCCoCr coating promotes a more uniform distribution of mechanical stresses during cavitation bubble collapse, leading to reduced surface degradation and extended service life.

Scratch test results indicate good adhesion of both coatings to the P250GH steel substrate. In both cases, no delamination was observed at the coating–substrate interface, and scratch widths were comparable for both the WCCoCr and CrCNi coatings. However, a notable difference was observed for the CrCNi coating, where microcracks parallel to the scratch axis appeared. This may indicate the presence of local stresses arising from significant hardness differences between phases in the coating, potentially reducing resistance under dynamic loading conditions such as cavitation.

Despite the higher microhardness of the CrCNi coating (904 HV0.2) compared to the WCCoCr coating (886 HV0.2), the WCCoCr coating exhibited better resistance to cavitation erosion. This indicates that microhardness is not the sole factor determining cavitation resistance—microstructure and the quality of inter-splat bonding also play a crucial role.

Final conclusion: Due to its favorable microstructural characteristics and higher resistance to cavitation-induced damage, the WCCoCr coating is more suitable for protecting the surfaces of machine and equipment components operating under intensive fluid flow conditions, particularly where long-term durability and operational reliability are critical.

References

[1] Kumar, K., Kumar, L. & Gill, H. (2024). Role of carbide-based thermal-sprayed coatings to prevent failure for boiler steels: a review. *Journal of Failure Analysis and Prevention*. 24(4), 1628-1663. DOI:10.1007/s11668-024-01974-y.

[2] Rodolpho, V., Silveira, L., Cruz, J. & Pukasiewicz, A. (2023). Cavitation resistance of FeMnCrSi coatings processed by different thermal spray processes. *Hybrid Advances*. 5, 100125, 1-18. DOI: 10.1016/j.hybadv.2023.100125.

[3] Cheng, F.T., Shi, P. & Man, H.C. (2001). Correlation of cavitation erosion resistance with indentation-derived properties for a NiTi alloy. *Scripta Materialia*. 45(9), 1083-1089. https://doi.org/10.1016/S1359-6462(01)01143-5.

[4] Stachowiak, G.B. & Stachowiak, G.W. (2010). Tribological characteristics of WC-based claddings using a ball-cratering method. *International Journal of Refractory Metals and Hard Materials*. 28(1), 95-105. https://doi.org/10.1016/j.ijrmhm.2009.07.015.

[5] Murthy, J.K.N. & Venkataraman, B. (2006). Abrasive wear behaviour of WC–CoCr and Cr3C2–20(NiCr) deposited by HVOF and detonation spray processes. *Surface and Coatings Technology*. 200(8), 2642-2652, https://doi.org/10.1016/j.surfcoat.2004.10.136.

[6] Yang, X., Zhang, J. & Li, G. (2016). Cavitation erosion behaviour and mechanism of HVOF-sprayed NiCrBSi–(Cr3C2–NiCr) composite coatings. *Surface Engineering*. 34(3), 211-219. https://doi.org/10.1080/02670844.2016.1258770.

[7] Matikainen, V., Koivuluoto, H. & Vuoristo, P. (2020). A study of Cr3C2-based HVOF-and HVAF-sprayed coatings: Abrasion, dry particle erosion and cavitation erosion resistance. *Wear*. 446-447, 203188, 1-11. https://doi.org/10.1016/j.wear.2020.203188.

[8] Silveira, L.L., Pukasiewicz, A.G.M., de Aguiar, D.J.M., Zara, A.J. & Björklund, S. (2019). Study of the corrosion and cavitation resistance of HVOF and HVAF FeCrMnSiNi and FeCrMnSiB coatings. *Surface and Coatings Technology.* 374, 910-922. https://doi.org/10.1016/j.surfcoat.2019.06.076.

[9] Nowakowska, M., Łatka, L., Sokołowski, P., Szala, M., Toma, F. & Walczak, M. (2022). Investigation into microstructure and mechanical properties effects on sliding wear and cavitation erosion of Al2O3–TiO2 coatings sprayed by APS, SPS and S-HVOF. *Wear*. 508-509, 204462, 1-15. https://doi.org/10.1016/j.wear.2022.204462.

[10] Odhiambo, J.G., Li, W., Zhao, Y. & Li, C. (2019). Porosity and its significance in plasma-sprayed coatings. *Coatings*. 9(7), 460, 1-19. https://doi.org/10.3390/coatings9070460.

[11] Sun, P., Fang, Z.Z., Zhang, Y. & Xia Y. (2017). Review of the methods for production of spherical Ti and Ti alloy powder. *JOM: the journal of the Minerals, Metals & Materials Society*. 69, 1853-1860. DOI: https://doi.org/10.1007/s11837-017-2513-5.

[12] Matikainen, V., Koivuluoto, H., Vuoristo, P., Schubert, J. & Houdková, Š. (2018). Effect of nozzle geometry on the microstructure and properties of HVAF-sprayed WC-10Co4Cr and Cr3C2-25NiCr coating. *Journal od Thermal Spray Technology*. 27(4), 680-694. DOI: 10.1007/s11666-018-0717-z.

[13] Houdková, Š., Zahálka, F., Kašparová, M. & Berger, L.M. (2011). Comparative study of thermally sprayed coatings under different types of wear conditions for hard chromium replacement. *Tribology Letters*. 43(2), 139-154. DOI: 10.1007/s11249-011-9791-9.

[14] Lugscheider, E., Barimani, C., Eckert, P. & Eritt, U. (1996). Modeling of the APS plasma spray process. *Computational Materials Science*. 7(1-2), 109-114. https://doi.org/10.1016/S0927-0256(96)00068-7.

[15] Wang, J., Wang, L., Lu, H., Du, J., Qi, X., Lu, L., Zhao, Y., Liu, Z. & Meng, W. (2025). Enhanced erosion resistance of Cr3C2-TiC-NiCrCoMo coatings: experimental and numerical investigation of erosion mechanisms. *Coatings*. 15(3), 294, 1-25. DOI: 10.3390/coatings15030294.

[16] Houdková, Š., Česánek, Z., Smazalová, E. & Lukáč, F. (2018). The high-temperature wear and oxidation behavior of CrC-based HVOF coatings. *Journal of Thermal Spray Technology*. 27(1), 179-195. DOI: 10.1007/s11666-017-0637-3.

[17] Padture, N.P., Gell, M., Jordan, E.H. (2002). Thermal barrier coatings for gas-turbine engine applications. *Science*. 296(5566), 280-284. DOI: 10.1126/science.1068609.

[18] Weeks, M.D., Subramanian, R., Vaidya, A. & Mumm, D.R. (2015). Defining optimal morphology of the bond coat–thermal barrier coating interface of air-plasma sprayed thermal barier coating systems. *Surface and coating technology*. 273, 50-59. DOI: 10.1016/j.surfcoat.2015.02.012.

[19] Sampath, S., Schulz, U., Jarligo, M.O. & Kuroda, S. (2012). Processing science of advanced thermal-barrier systems. *MRS Bulletin*. 37(10), 903-910. DOI: 10.1557/mrs.2012.233.

[20] Mutter, M., Mauer, G., Mücke, R., Guillon, O. & Vaßen, R. (2017). Correlation of splat morphologies with porosity and residual stress in plasma-sprayed YSZ coating. *Surface and coating technology*. 318, 157-169. https://doi.org/10.1016/j.surfcoat.2016.12.061.

[21] McPherson, R. (1989). A review of microstructure and properties of plasma sprayed ceramic coatings. *Surface and coating technology*. 39-40(1), 173-181. https://doi.org/10.1016/0257-8972(89)90052-2.